JOC The Journal of Organic Chemistry
Article
pubs.acs.org/joc

Theoretical Study on the Regioselectivity of Baeyer–Villiger Reaction of α-Me-, -F-, -CF$_3$-Cyclohexanones

Yoshimitsu Itoh,[†] Masahiro Yamanaka,[‡] and Koichi Mikami*

Department of Applied Chemistry, Tokyo Institute of Technology, Tokyo 152-8552, Japan

Ⓢ *Supporting Information*

ABSTRACT: The origin of the regioselectivity of the Baeyer–Villiger reaction of α-Me-, -F-, and -CF$_3$-cyclohexanones was investigated theoretically (MPWB1K/6-311++G**-PCM(CH$_2$Cl$_2$)//MPWB1K/6-311G**-Onsager-(CH$_2$Cl$_2$)). Investigation of the energy profiles of the rearrangement step revealed the reality of the importance of conventional migratory aptitude based on the stabilization capability of partial positive charge generated during the migration step. We have divided the origin of the regioselectivity into two factors: (1) structural stability (steric repulsion, dipole interaction, etc.) and kinetic reactivity (energy barrier from the intermediate, i.e., cation stabilization capability). For α-CF$_3$-cyclohexanone, the migration tendency was mostly dependent on the kinetic reactivity; CF$_3$ substitution greatly increased the energy barrier. Noteworthy is the orientation of the CF$_3$ group at the transition state. The CF$_3$ group possessed the axial orientation overcoming the 1,3-diaxial repulsion, probably because of the strong dipole interaction between the CF$_3$ group and the leaving acid moiety. Striking results in the case of α-F- and -Me-cyclohexanone were that no difference in the energy barriers by the substituents could be observed. Especially in the case of α-Me substitution, structural stability operates in determining the most stable transition state, which is in contrast to the conventional understanding of the migratory aptitude based on the ability to stabilize partial positive charge.

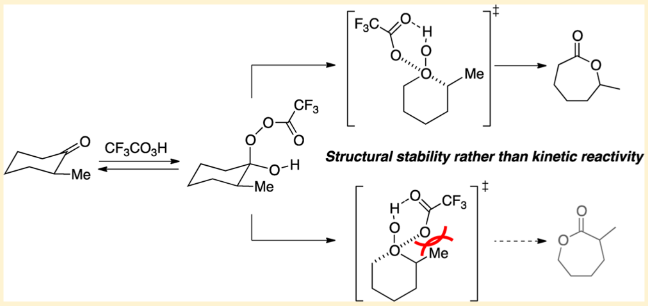

■ INTRODUCTION

The Baeyer–Villiger (B–V) reaction[1] has been widely employed in organic synthesis by virtue of the unique transformation; an oxygen atom can be inserted regioselectively and stereospecifically into a carbon–carbon single bond.[2,3] A two-step mechanism has been well-accepted: (1) carbonyl addition of a peroxy acid to form a peroxy acid/carbonyl adduct, the so-called Criegee intermediate,[4] and then (2) skeletal rearrangement thereof to give lactones or esters. Many kinetic studies[5] had been carried out to reveal that rearrangement of the Criegee intermediate is a concerted process and, with some exceptions,[5f,i] a rate-determining step (Figure 1).

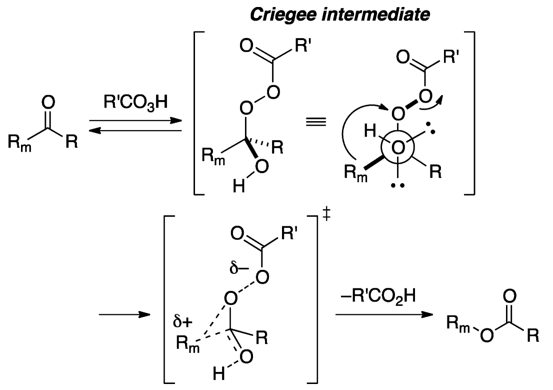

Figure 1. Primary stereoelectronic effect in the Criegee intermediate.

The regioselectivity has long been the most important issue in the B–V reaction. Regioselectivity is normally highly predictable. Migratory aptitude decreases in the order: tertiary alkyl > secondary alkyl > primary alkyl > methyl.[2b] It is widely believed that the ketonic substituent that can best stabilize a partial positive charge at the transition state of the migration step usually migrates preferentially. It has also been well-accepted that the stereoelectronic requirement for correct *anti*-periplanar alignment of the migrating substituent and the O–O bond of the leaving peroxy acid (e.g., R′COO$^-$), referred to as the primary stereoelectronic effect, is required at the migrating step (Figure 1).[6] Such a primary stereoelectronic effect has been rationalized, though in few reports, where the migration of the carbon **a** is located in correct *anti*-periplanar alignment by (i) conformational requirements[7] or (ii) stereoelectronic requirements by the dipole interaction (Figure 2).[8] In Chandrasekhar's model (Figure 2i), the conformation of the Criegee intermediate is fixed by the rigid bicyclic system, and thus the C–O bond which is in *anti*-periplanar alignment was the only choice for migration. Crudden's model (Figure 2ii) gives a striking demonstration of the operation of primary stereoelectronic effect. When the F group is in equatorial

Special Issue: Robert Ireland Memorial Issue

Received: October 1, 2012
Published: November 28, 2012

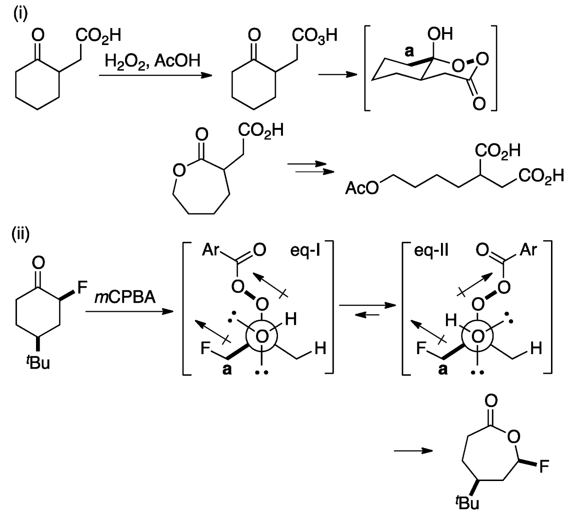

Figure 2. Primary stereoelectronic effect in the Criegee intermediate of (i) Chandrasekhar's and (ii) Crudden's models.

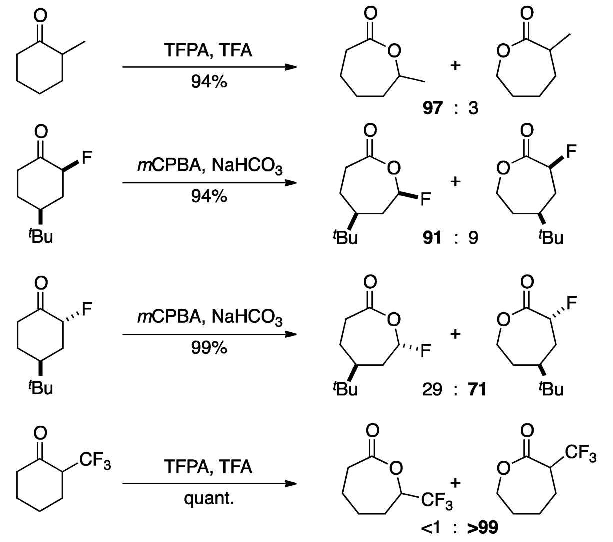

Figure 3. B−V reaction of α-Me-, -F-, and -CF_3-cyclohexanone.

orientation, as shown in Figure 2ii, dipole interaction between the C−F bond and the leaving acid moiety destabilizes the conformation of eq-I of the Criegee intermediate, making it easier for the C−F group to migrate. Opposite migration tendency was observed with low selectivity when the F group was in axial orientation. In these experiments, primary stereoelectronic effect controls the regioselectivity rather than the conventional migratory aptitude based on cation stabilization. Considering the regioselectivity of the B−V reaction, we learn from the discussion above that the first thing is to construct all possible conformations in the Criegee intermediate, which fulfills the correct *anti*-periplanar alignment, and then compare the stability of the following transition state considering both structural stability (steric repulsion, dipole interaction, etc.) or kinetic reactivity (energy barrier from the intermediate, i.e., cation stabilization capability). The reaction finally proceeds from the most stable transition state, as the transition state is the expression of the whole energetics stated above, and the regioselectivity depends on the energies of the transition state.

Recently, we reported the B−V reaction of α-CF_3-cyclohexanone and observed the exclusive migration of the carbon without the CF_3 group.[9] Since the CF_3 group has a strong electron-withdrawing nature, the regioselectivity could be explained by the conventional migratory aptitude. It was found by theoretical investigation that the most stable transition state bears a sterically demanding CF_3 group in axial orientation normally unfavorable due to the 1,3-diaxial repulsion. This is attributable to the interaction of two dipole moments from the α-CF_3 group and the leaving group.

The experimental result of the regioselectivity of α-Me,[10] -F-,[8] and -CF_3[9]-cyclohexanone is shown in Figure 3. It is interesting to note that the regioselectivity of α-Me-cyclohexanone, a typical example of B−V reaction, is considered to be dependent on the conventional migratory aptitude based on cation stabilization. No further investigation on the regioselectivity has been conducted to date.

The focus of this paper is the computational exploration on the origin of the regioselectivity of the B−V reaction of cyclohexanone derivatives, as they are a typical substrate for the B−V reaction, especially focusing on the effect of α-substituents. Although a lot of computational investigation of the B−V reaction has been carried out,[11] most of them discuss the mechanism of the whole reaction process and not the regioselectivity, except for the one reported by Grein et al., which showed the energetic difference caused by α-halo substitution.[11n] By investigating the migration step of all possible conformations for each substrate, we successfully clarified the role of the two factors controlling the regioselectivity. It was revealed, to our surprise, that, in the case of α-Me-cyclohexanone, regioselectivity did not depend on the difference in energy barrier from the intermediate caused by the methyl substitution but rather on the structural stability based on the steric repulsion between the α-substituent and the leaving acid moiety. This investigation will lead to a further understanding of the origin of the regioselectivity of the B−V reaction.

■ CHEMICAL MODELS AND COMPUTATIONAL METHODS

The regioselectivity of the B−V reaction is determined at the stage of the migration step from the Criegee intermediate. Therefore, the Criegee intermediate and the transition state of the migration step of the B−V reaction of cyclohexanone derivatives with trifluoroperacetic acid (TFPA) were optimized.

When calculating the mechanism of the B−V reaction, we need to consider how to take into account the effect of the coexisting acid. The effect of the acid on the structure of the reaction pathway has been investigated extensively, but different models and calculation levels often lead to different conclusions.[11c,n,o,q−u,w,x] Recently, Alvarez−Idaboy et al. reported a theoretical study on the whole reaction pathway of the B−V reaction of propanone and cyclohexanone with trifluoroperacetic acid and compared their result to the experimental kinetic studies.[11s] The calculation result showed a good agreement with the kinetic data. Their proposed mechanism is acid-catalyzed addition of peracid to ketone followed by noncatalyzed migration (Figure 4). The calculation level they employed is high enough (MPWB1K/6-311++G**-PCM(CH_2Cl_2)//MPWB1K/6-311G**-Onsager(CH_2Cl_2)) compared to the previous theoretical investigations.[11] We think that this model and calculation method is so far the best to follow in our study.

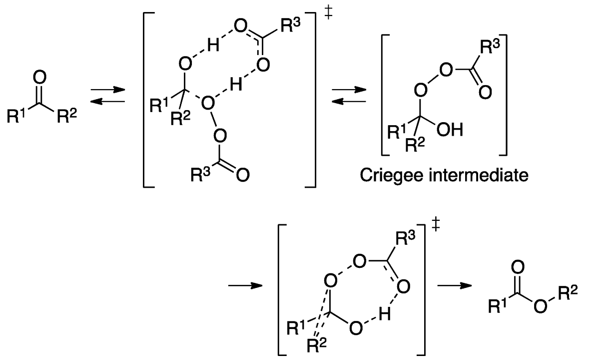

Figure 4. Proposed mechanism and the effect of acid for the B–V reaction by Alvarez–Idaboy.

Previously, we reported the theoretical investigation of the migration step of the B–V reaction of α-CF_3-cyclohexanone.[9] The calculation method we used at that time was MP2/6-31G**//HF/6-31G* level according to the report by Okuno.[11c] In this report, we decided to revisit all of the structures according to the report by Alvarez–Idaboy et al.[11s] Although there was no significant change to the conclusion reported in our previous study, we believe that the new method gives more accurate energetics.

As shown in Figure 5, there are a total of eight possible conformations in the rearrangement step with respect to the orientation (axial or equatorial) of the oxidant and R group and the regioselectivity of the migrating carbon (path ***a*** or ***b***). All of the structures of the Criegee intermediates (**CPs**) and the transition states (**TSs**) from the corresponding intermediates were calculated for each X = Me, F, and CF_3 substituent.

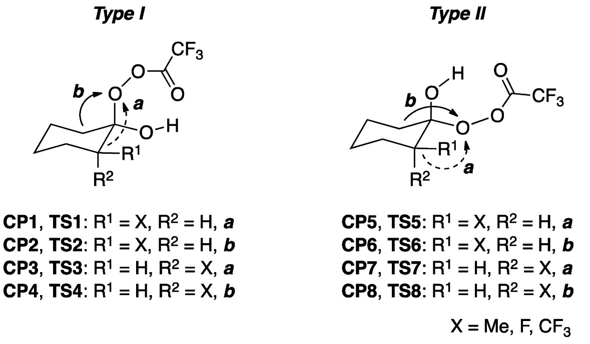

Figure 5. Chemical model of the B–V reaction.

All of the calculations were performed with the Gaussian 09[12] program package. The structures were first optimized with B3LYP/6-31+G**[13,14] under vacuum. Then, starting from the optimized structures, it was reoptimized at MPWB1K/6-311G**[15] with the Onsager solvent model (CH_2Cl_2, ε = 8.93)[16] followed by frequency calculation at the same level. All the **CPs** and **TSs** were confirmed to have zero and one imaginary frequency, respectively. Then, single-point energy and frequency calculations were carried out in the presence of a polarizable dielectric (CH_2Cl_2, ε = 8.93) as described by the IEF-PCM model[17] at the MPWB1K/6-311++G** level. The energies shown in this report are the Gibbs free energies of the results of final single-point calculations containing zero-point, thermal, and entropy effects at 298.15 K. Natural charges were calculated by the natural population analysis[18] at the same level of the theory used for the final single-point calculations.

RESULTS AND DISCUSSION

α-CF_3-Cyclohexanone. Relative Gibbs free energies based on the most stable **CP** for all eight possible conformations of CPs and TSs for α-CF_3-cyclohexanones are listed in Table 1 and shown graphically in Figure 6. Calculation of the product distribution from the energies of the transition states based on Boltzmann distribution gave ***a***/***b*** = 6:94, showing good agreement with the experimental result. The energy diagram in Figure 6 looks, at a glance, complicated and difficult to analyze because of the small energy difference. However, there is an obvious tendency when focusing on the energy barriers from the intermediates: the ***a*** series have larger energies than the ***b*** series. The range of the energy barrier could be clearly distinguished from ***a*** series with the range being between 23.8 and 26.2 kcal/mol, and ***b*** series being between 19.6 and 22.9 kcal/mol. It is clear from the gradient of the line connecting CPs and TSs in the energy diagram (Figure 6) that the ***a*** series (dotted line) have a gradient larger than that of the ***b*** series (solid line). This is obviously because of the strong electron-withdrawing nature of the CF_3 group. Partial positive charge generated on the migrating carbon during the reaction pathway will be destabilized by the CF_3 group, leading to the higher energy barrier. Thus the conventional understanding of migratory aptitude based on kinetic reactivity (energy barrier from the intermediate) operates here.

Table 1. Relative Gibbs Free Energies of CF_3-CPs and CF_3-TSs at the MPWB1K/6-311++G-PCM(CH_2Cl_2)//MPWB1K/6-311G**-Onsager(CH_2Cl_2) Level**

Type I	ΔG_{CP} (kcal/mol)		ΔG_{TS} (kcal/mol)	$\Delta G_{TS}-\Delta G_{CP}$ (kcal/mol)
CF_3-**CP1**	0.0	CF_3-**TS1**	24.0	24.0
CF_3-**CP2**	3.9	CF_3-**TS2**	23.8	19.9
CF_3-**CP3**	2.3	CF_3-**TS3**	28.5	26.2
CF_3-**CP4**	0.8	CF_3-**TS4**	22.4	21.6
Type II	ΔG_{CP} (kcal/mol)		ΔG_{TS} (kcal/mol)	$\Delta G_{TS}-\Delta G_{CP}$ (kcal/mol)
CF_3-**CP5**	0.2	CF_3-**TS5**	25.4	25.2
CF_3-**CP6**	4.2	CF_3-**TS6**	23.8	19.6
CF_3-**CP7**	3.0	CF_3-**TS7**	26.8	23.8
CF_3-**CP8**	1.1	CF_3-**TS8**	24.0	22.9

Special note should be given to the orientation of the CF_3 group. **CF_3-TS4**, the most stable transition state, has a CF_3 group on the axial orientation. What causes the sterically demanding CF_3 to possess axial orientation, which is usually less preferred because of 1,3-diaxial repulsion? We attributed this phenomenon to the stabilization by dipole interaction between the CF_3 group and the leaving trifluoroacetate moiety.[9] When looking at the structure of the transition state, the most stable transition state **CF_3-TS4** has the CF_3 group in an axial orientation and the trifluoroacetate group is in nearly *anti*-parallel (128°) orientation from the CF_3 group (Figure 7). We think that cancellation of the dipole moments stabilizes **CF_3-TS4**. By comparing the structure of **CF_3-TS4** with that of **CF_3-TS2**, which is in the same ***b*** series with **CF_3-TS4** but with

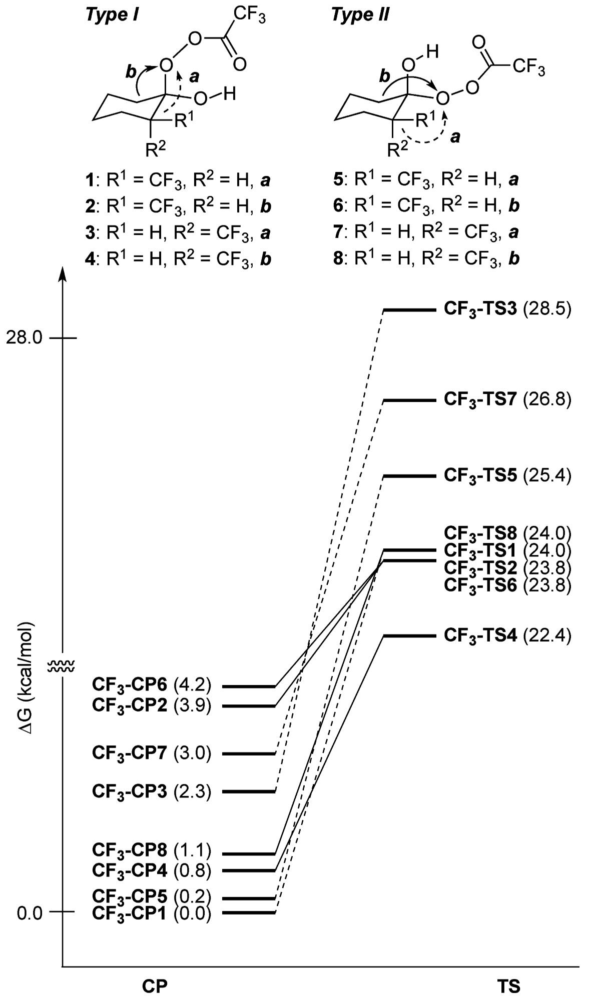

Figure 6. Energy diagram of the rearrangement step of α-CF_3-cyclohexanone in terms of ΔG (kcal/mol).

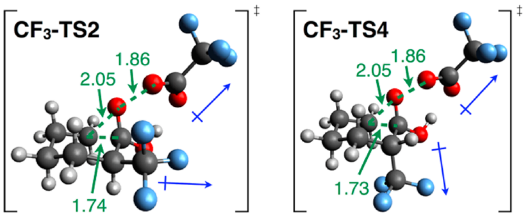

Figure 7. Three-dimensional structure of **CF_3-TS2**, **CF_3-TS4** (carbon, black; hydrogen, gray; oxygen, red; blue, blue). The numbers refer to the distances in Å.

the CF_3 group in an equatorial orientation, the effect of dipole cancellation is more clear because the trifluoroacetate group is at an angle of 42° from the CF_3 group in **CF_3-TS2**, resulting in higher energy.

α-F-Cyclohexanone. Energy profile for the reaction of α-F-cyclohexanones (Figure 8, Table 2) was relatively featureless compared to that of α-CF_3-cyclohexanones. All of the energies of **CP**s were within only 2.9 kcal/mol difference, and those of **TS**s were within only 2.7 kcal/mol difference. Experimental product yield for the B–V reaction of α-F-cyclohexanone using *m*CPBA was reported for the substrate with fixed F orientation by a bulky *t*-Bu group, as shown in Figure 3.[8] For the substrate with the F group in the equatorial orientation (**F_eq**: **1**, **2**, **5**, **6**), calculation of the product distribution based on the Boltzmann distribution from the energies of the transition state gave ***a***/***b*** = 74:26, and the same calculation for the F group in the axial orientation (**F_ax**: **3**, **4**, **7**, **8**) gave ***a***/***b*** = 29:71. This value is in good agreement with the experimental results, which were 91:9 for **F_eq** and 29:71 for **F_ax**, showing the reliability of the calculation results.

In stark contrast to α-CF_3-cyclohexanone, the energy barriers from the intermediates for all of the α-F-cyclohexanones were within only 2.7 kcal/mol, and the dependency of the energy barriers on the F substitution is not significant. This means that the direct electronic effect of F substitution on the α-carbon does not affect the migratory aptitude, and the stereoelectronic factor plays a more important role, which is consistent with the proposal by Crudden et al.[8] where the primary stereoelectronic

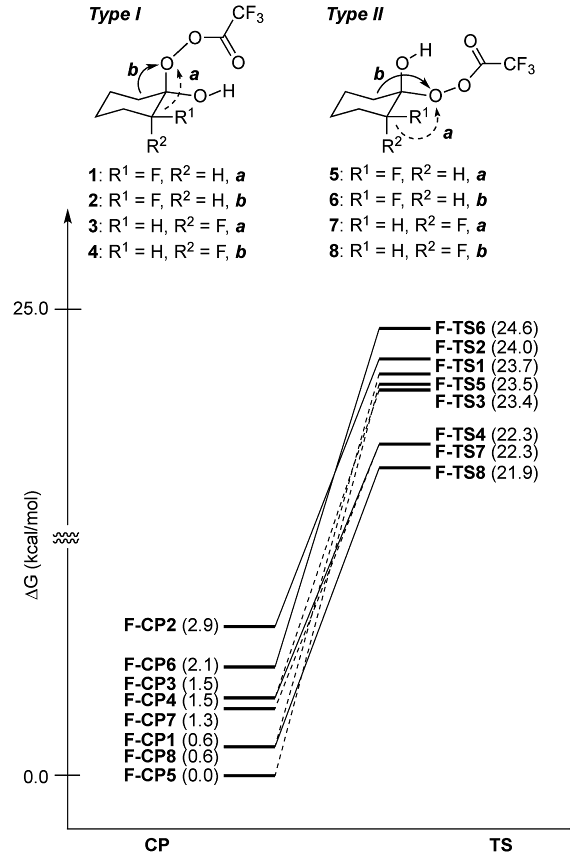

Figure 8. Energy diagram of the rearrangement step of α-F-cyclohexanone in terms of ΔG (kcal/mol).

Table 2. Relative Gibbs Free Energies of F-CPs and F-TSs at the MPWB1K/6-311++G-PCM(CH_2Cl_2)//MPWB1K/6-311G**-Onsager(CH_2Cl_2) Level**

Type I	ΔG_{CP} (kcal/mol)		ΔG_{TS} (kcal/mol)	$\Delta G_{TS}-\Delta G_{CP}$ (kcal/mol)
F-CP1	0.6	F-TS1	23.7	23.1
F-CP2	2.9	F-TS2	24.0	21.1
F-CP3	1.5	F-TS3	23.4	21.9
F-CP4	1.5	F-TS4	22.3	20.8
Type II	ΔG_{CP} (kcal/mol)		ΔG_{TS} (kcal/mol)	$\Delta G_{TS}-\Delta G_{CP}$ (kcal/mol)
F-CP5	0.0	F-TS5	23.5	23.5
F-CP6	2.1	F-TS6	24.6	22.5
F-CP7	1.3	F-TS7	22.3	21.0
F-CP8	0.6	F-TS8	21.9	21.3

effect works predominantly in determining the regioselectivity of the B−V reaction of *α*-F-cyclohexanone (Figure 2ii). Crudden et al. emphasized the importance of the dipole interaction between the C−F bond and the leaving acid moiety as the determining factor of regioselectivity in the case of the **F_eq** substrate. If we compare the energies of **F-CP1** and **F-CP2**, which correspond to eq-I and eq-II in Figure 2ii, it is largely different by 2.3 kcal/mol. Since the angles between the F group and the leaving acid group (*θ*) in **F-CP1** and **F-CP2** are 108 and 13°, respectively, the stability of **F-CP1** could be attributed to cancellation of dipole moments of the two groups (Figure 9). In fact, the total dipole moments of **F-CP1** and **F-CP2** are 5.2 and 5.8 D, respectively (Table 3), which is in good agreement with the discussion of dipole cancellation. In the transition state, the energy difference decreased to 0.3 kcal/mol. This significant decrease is attributable to the change in the *θ* value (84° for **F-TS1** and 38° for **F-TS2**) which lowers the structural stabilization by dipole cancellation effect and thus leads the energies of **F-TS1** and **F-TS2** closer. The same discussion could be done in the structure with the acid moiety in an equatorial orientation (**F-CP5** and **F-CP6**). **F-CP5** has higher *θ* value (106°) and thus lower dipole molent (5.5 D), leading to lower energy compared to **F-CP6** (*θ* = 16°, dipole moment = 5.9 D). It is interesting to note that **F_eq** series has higher transition state energy than **F_ax** series. By looking at the dipole moment of the transition state (Table 3), we can find a clear relationship between the energy tendency and the dipole moment; dipole moment of the **F_eq** series is larger than the **F_ax** series.

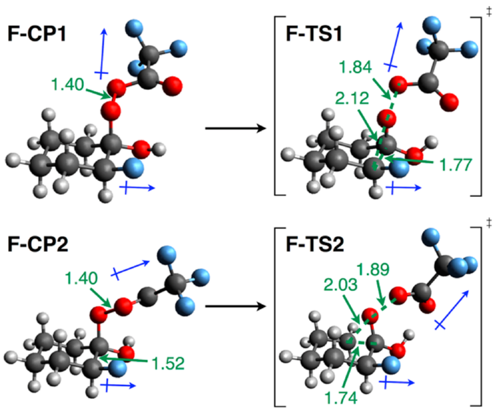

Figure 9. Three-dimensional structures of **F-CP1**, **CP2**, **F-TS1**, and **TS2** (carbon, black; hydrogen, gray; oxygen, red; blue, blue). The numbers refer to the distances in Å.

Table 3. Dipole Moment of F-CPs and F-TSs

F		dipole moment (D)		dipole moment (D)
eq.	**F-CP1**	5.2	**F-TS1**	9.8
eq.	**F-CP2**	5.8	**F-TS2**	11.4
ax.	**F-CP3**	3.1	**F-TS3**	8.3
ax.	**F-CP4**	3.4	**F-TS4**	8.5
eq.	**F-CP5**	5.5	**F-TS5**	10.2
eq.	**F-CP6**	5.9	**F-TS6**	11.8
ax.	**F-CP7**	3.4	**F-TS7**	9.1
ax.	**F-CP8**	4.0	**F-TS8**	9.1

From the discussion above, the regioselectivity of the *α*-F-cyclohexanone is mostly dependent on the dipole interaction between the dipole from the C−F bond and the leaving acid moiety. Stereoelectronic stability (structural stability) is the determining factor, and the partial cation stabilization is not operating here.

***α*-Me-Cyclohexanone.** Among all of the investigations reported here, analysis of the regioselectivity of *α*-Me-cyclohexanone was the most impressive one since this substrate is often used as an example to explain the regioselectivity of the B−V reaction. As discussed later, the commonly accepted migratory aptitude by cation stabilization does not operate here.

Energetics of all possible conformations are described in Table 4 and graphically shown as an energy diagram in Figure 10. Calculation of the product distribution using Boltzmann distribution was ***a***/***b*** = 6:94. By comparing with the experimental result (Figure 3, ***a***/***b*** = 3:97), again, we can be confident about the calculation level.

Table 4. Relative Gibbs Free Energies of Me-CPs and Me-TSs at the MPWB1K/6-311++G-PCM(CH_2Cl_2)//MPWB1K/6-311G**-Onsager(CH_2Cl_2) Level**

Type I	ΔG_{CP} (kcal/mol)		ΔG_{TS} (kcal/mol)	$\Delta G_{TS}-\Delta G_{CP}$ (kcal/mol)
Me-CP1	2.0	**Me-TS1**	19.0	17.0
Me-CP2	5.5	**Me-TS2**	21.5	16.0
Me-CP3	2.2	**Me-TS3**	20.1	17.9
Me-CP4	2.3	**Me-TS4**	20.9	18.6
Type II	ΔG_{CP} (kcal/mol)		ΔG_{TS} (kcal/mol)	$\Delta G_{TS}-\Delta G_{CP}$ (kcal/mol)
Me-CP5	0.0	**Me-TS5**	19.7	19.7
Me-CP6	4.0	**Me-TS6**	21.3	17.3
Me-CP7	3.6	**Me-TS7**	20.3	16.7
Me-CP8	2.3	**Me-TS8**	21.7	19.4

The first thing to point out in the energy diagram for the migration step of *α*-Me-cyclohexanone (Figure 10) is the transition state. Energetics of the transition state could be separated in the middle, where all of the lower energy transition states (**1**, **5**, **3**, **7**) are ***a*** series (migration of CHMe) and the rest of the transition states (**4**, **6**, **2**, **8**) are ***b*** series (migration of CH_2). Distinct from *α*-CF_3- and *α*-F-cyclohexanone, migration of Me-substituted carbon is predominant, no matter what the orientation is. We first thought that this is because of the stabilization of partial positive charge by the Me group. However, it was difficult to find a tendency in the energy barrier from the intermediate based on *α*-Me substitution, where all energy barriers are within 3.7 kcal/mol difference. This means that stabilization of partial positive charge is not controlling the regioselectivity. When we turn the attention to the Criegee intermediate (CPs), we can find that most of the lower energy structure is the complex leading to CHMe migration, in accordance with the tendency found in the energy level of the transition state. This observation shows that it is not the stabilization of partial positive charge by the Me substituent that determines the regioselectivity, but other structural factors commonly observed both in the intermediate and in the transition state play an important role.

Structures of **Me-TS1** and **Me-TS2** are shown in Figure 11. It could be easily recognized that the leaving acid moiety points toward the Me-substituted carbon in all of the ***b*** series. This is

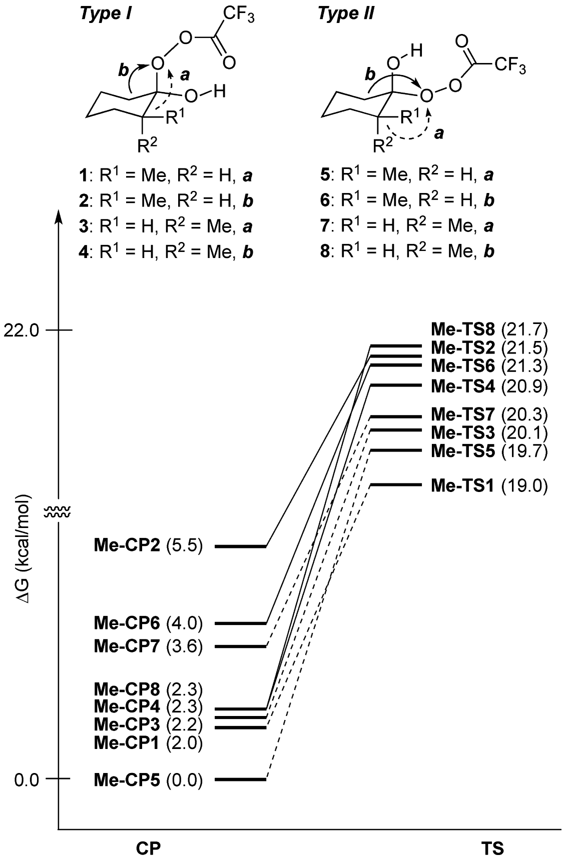

Figure 10. Energy diagram of the rearrangement step of α-Me-cyclohexanone in terms of ΔG (kcal/mol).

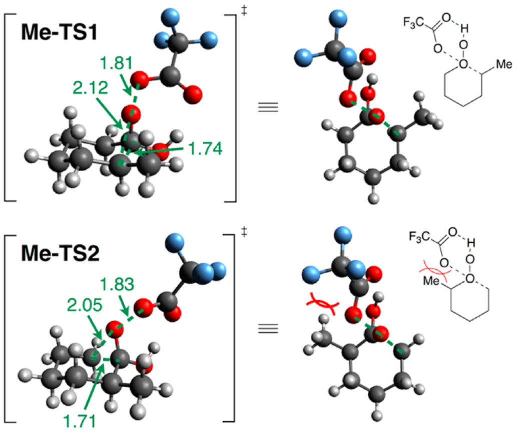

Figure 11. Three-dimensional structure of **Me-TS1** and **Me-TS2** (carbon, black; hydrogen, gray; oxygen, red; blue, blue). The numbers are the distances in Å.

actually the result when the structure tries to meet the requirement of primary stereoelectronic effect since the α-carbon attacks the O–O bond from the backside of the acid moiety. Therefore, it could be said that the sterically hindered substituent on the α-carbon migrates preferentially in order to avoid the steric repulsion between the leaving acid moiety. In fact, for the alkyl group, the order of the *A* value (e.g., *t*-Bu (>4) > *i*-Pr (2.15) > Et (1.75) > Me (1.70))[19] is in the same order of empirical migratory aptitude.

When the orientation of the Me group is in axial orientation (**Me_ax**: **3**, **4**, **7**, **8**), one might think that steric repulsion between the leaving acid moiety is less significant compared to the structure with the Me group in an equatorial orientation (**Me_eq**: **1**, **2**, **5**, **6**). In fact, the energy barrier for **CP3**-to-**TS3** (CHMe migration, 17.9 kcal/mol) is smaller than that of **CP4**-to-**TS4** (CH_2 migration, 18.6 kcal/mol). The same tendency is observed for the energy barrier for **CP7**-to-**TS7** and **CP8**-to-**TS8**. In these cases, stabilization of partial cation by the Me group might be working. However, since 1,3-diaxial repulsion raises all of the energetics of the **Me_ax** series, these structures could not be the most stable transition state to determine the regioselectivity.

Group Charges. We have carried out a comparison between the group charges of the migrating group (CHX or CH_2) and the energy barriers from the intermediates and found a clear relationship with the discussions above. When looking at the group charge, which is the sum of the atomic NPA charges in the migrating group, it is more cationic in the transition state than in the intermediate no matter what the α-substituent is (Supporting Information, Table S1). Figure 12 shows a plot of NPA charges of the migrating groups versus energy barriers from the intermediate for each α-substituent. For the plot of α-CF_3-cyclohexanone, it is clear that migration of $CHCF_3$ has an energy barrier higher that that of CH_2 migration, and moreover, group charge for $CHCF_3$ and for CH_2 is distinctly separated (Figure 12). This clear relationship is only observed for the α-CF_3 case, and it is rather unclear for the α-F and α-Me cases. In the previous discussions, it was understood that only the case of α-CF_3 regioselectivity could be explained by the conventional understanding based on cation stabilization capability. This is now reinforced by the discussion of the group charge and the energy barrier, which has the same tendency. Bond distance transitions from the intermediate to the transition state are shown in Table S2 (Supporting Information). From this table, especially from the column of $d^1_{TS}-d^1_{CP}$, the transition state structure of α-Me substrates is relatively early compared to that of α-CF_3 substrates, and α-F substrates are rather close to α-CF_3 substrates. When the stability of the transition state is related to cation stabilization or dipole moment relaxation (α-CF_3 and α-F), late transition state gives more pronounced difference in the transition state energies because, as the reaction proceeds, the charge and the dipole moment will have a large difference from the intermediates. This is what we have observed in the case of α-CF_3 and α-F substrates. Early transition state in α-Me substrates explains the less direct electronic effect from α-Me substituents since the cation generation is low at the early stage of the reaction.

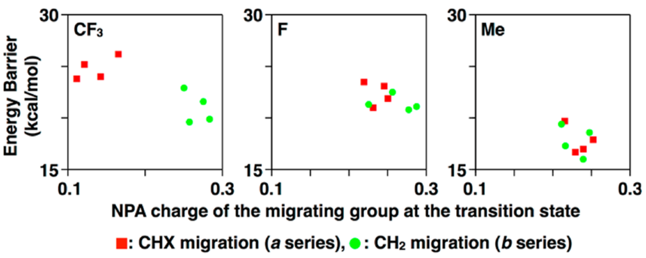

Figure 12. Plot of the migrating group charge at the transition state. The group charge is a sum of the atomic charges in the migrating group obtained by the natural population analysis.

CONCLUSION

The regioselectivity of the B−V reaction of α-Me-, -F-, and -CF_3-cyclohexanones was investigated theoretically to reveal the importance of the conventional migratory aptitude based on partial cation stabilization. It was clarified that only in the case of CF_3 substitution that the cation stabilization really works for determining the regioselectivity. In the case of α-CF_3-cyclohexanone, the energy barrier for the $CHCF_3$ migration was obviously higher than the CH_2 migration. For α-F- and -Me-cyclohexanone, there was no significant difference in energy barrier among the different substitution and orientation of the substituents. Further investigation revealed that dipole cancellation affects the regioselectivity of α-F-cyclohexanone. For α-Me-cyclohexanone, the origin of the migratory aptitude was concluded to be a steric repulsion between the α-Me group and the leaving acid moiety rather than the cation stabilization effect. Our investigation shows that unless a substituent with very strong electron-withdrawing nature is introduced at the α-positon to the carbonyl group, which would strongly destabilize the partial cation, the regioselectivity will be more affected by the structural stability. Although it is too early to make a general conclusion, the conventional understanding of the role of cation stabilization in the migratory aptitude might need some revision based on steric repulsion.

ASSOCIATED CONTENT

Supporting Information

NPA charges of the migrating group, bond length transitions from the intermediate to the transition state, molecular geometries and energies for the optimized stationary points. This material is available free of charge via the Internet at http://pubs.acs.org.

AUTHOR INFORMATION

Corresponding Author

*E-mail: mikami.k.ab@m.titech.ac.jp.

Present Addresses

[†]Department of Chemistry and Biotechnology, School of Engineering, The University of Tokyo, Tokyo 113-8656, Japan.
[‡]Department of Chemistry, Rikkyo University, Tokyo 171-8501, Japan.

Notes

The authors declare no competing financial interest.

ACKNOWLEDGMENTS

Generous allotment of computational time from the Institute for Molecular Science, Okazaki, Japan is greatly acknowledged.

DEDICATION

Dedicated to the late Professor Robert E. Ireland to perpetuate his memory.

REFERENCES

(1) Baeyer, A.; Villiger, V. *Ber. Dtsch. Chem. Ges.* **1899**, *32*, 3625−3633.

(2) Reviews: (a) Krow, G. R. In *Comprehensive Organic Synthesis*; Trost, B. M., Ed.; Pergamon: Oxford, 1991; Vol. 7, p 671. (b) Krow, G. R. *Org. React.* **1993**, *43*, 251−798. (c) Strukul, G. *Angew. Chem., Int. Ed.* **1998**, *37*, 1198−1209. (d) Renz, M.; Meunier, B. *Eur. J. Org. Chem.* **1999**, 737−750. (e) Brink, G.-J.; ten Arends, I. W. C. E.; Sheldon, R. A. *Chem. Rev.* **2004**, *104*, 4105−4123.

(3) (a) Ireland, R. E.; Maienfisch, P. *J. Org. Chem.* **1988**, *53*, 640−651. (b) Ireland, R. E. *Aldrichimica Acta* **1988**, *21*, 59−69 and the references cited therein.

(4) Criegee, R. *Justus Liebigs Ann. Chem.* **1948**, *560*, 127−135.

(5) (a) Friess, S. L.; Soloway, A. H. *J. Am. Chem. Soc.* **1951**, *73*, 3968−3972. (b) Hawthorne, M. F.; Emmons, W. D. *J. Am. Chem. Soc.* **1958**, *80*, 6398−6404. (c) Ogata, Y.; Sawaki, Y. *J. Org. Chem.* **1969**, *34*, 3985−3991. (d) Palmer, B. W.; Fry, A. *J. Am. Chem. Soc.* **1970**, *92*, 2580−2581. (e) Ogata, Y.; Sawaki, Y. *J. Am. Chem. Soc.* **1972**, *94*, 4189−4196. (f) Ogata, Y.; Sawaki, Y. *J. Org. Chem.* **1972**, *37*, 2953−2957. (g) Winnik, M. A.; Stoute, V. *Can. J. Chem.* **1973**, *51*, 2788−2793. (h) Winnik, M. A.; Stoute, V.; Fitzgerald, P. *J. Am. Chem. Soc.* **1974**, *96*, 1977−1979. (i) Singleton, D. A.; Szymanski, M. J. *J. Am. Chem. Soc.* **1999**, *121*, 9455−9456.

(6) Correct *anti*-periplanar alignment of the lone electron pair of the hemiacetal oxygen and the migrating substituents (secondary stereoelectronic effect) is also proposed for the migration step. (a) Noyori, R.; Sato, T.; Kobayashi, H. *Tetrahedron Lett.* **1980**, *21*, 2569−2572. (b) Noyori, R.; Kobayashi, H.; Sato, T. *Tetrahedron Lett.* **1980**, *21*, 2573−2576.

(7) Chandrasekhar, S.; Roy, C. D. *Tetrahedron Lett.* **1987**, *28*, 6371−6372.

(8) Crudden, C. M.; Chen, A. C.; Calhoun, L. A. *Angew. Chem., Int. Ed.* **2000**, *39*, 2852−2855.

(9) Itoh, Y.; Yamanaka, M.; Mikami, K. *Org. Lett.* **2003**, *5*, 4803−4806.

(10) The experiment was carried out according to the procedure described in ref 9 using 2-methylcyclohexanone. The product distribution was determined by ^1H NMR and GC analysis.

(11) (a) Stoute, V. A.; Winnik, M. A.; Csizmadia, I. G. *J. Am. Chem. Soc.* **1974**, *96*, 6388−6393. (b) Cárdenas, R.; Cetina, R.; Lagúnez-Otero, J.; Reyes, L. *J. Phys. Chem. A* **1997**, *101*, 192−200. (c) Okuno, Y. *Chem.—Eur. J.* **1997**, *3*, 212−218. (d) Hannachi, H.; Anoune, N.; Arnaud, C.; Lantéri, P.; Longeray, R.; Chermette, H. *J. Mol. Struct.* **1998**, *434*, 183−191. (e) Cádenas, R.; Reyes, L.; Lagúnez-Otero, J.; Cetina, R. *J. Mol. Struct.* **2000**, *497*, 211−225. (f) Lehtinen, C.; Nevalainen, V.; Brunow, G. *Tetrahedron* **2000**, *56*, 9375−9382. (g) Carlqvist, P.; Eklund, R.; Brinck, T. *J. Org. Chem.* **2001**, *66*, 1193−1199. (h) Lehtinen, C.; Nevalainen, V.; Brunow, G. *Tetrahedron* **2001**, *57*, 4741−4751. (i) Carlqvist, P.; Eklund, R.; Hult, K.; Brinck, T. *J. Mol. Model.* **2003**, *9*, 164−171. (j) Sever, R. R.; Root, T. W. *J. Phys. Chem. B* **2003**, *107*, 10848−10862. (k) Snowden, M.; Bermudez, A.; Kelly, D. R.; Radkiewicz-Poutsma, J. L. *J. Org. Chem.* **2004**, *69*, 7148−7156. (l) Boronat, M.; Corma, A.; Renz, M.; Sastre, G.; Viruela, P. M. *Chem.—Eur. J.* **2005**, *11*, 6905−6915. (m) Reyes, L.; Castro, M.; Cruz, J.; Rubio, M. *J. Phys. Chem. A* **2005**, *109*, 3383−3390. (n) Grein, F.; Chen, A. C.; Edwards, D.; Crudden, C. M. *J. Org. Chem.* **2006**, *71*, 861−872. (o) Alvarez-Idaboy, J. R.; Reyes, L.; Cruz, J. *Org. Lett.* **2006**, *8*, 1763−1765. (p) Kovács, A.; Nemcsok, D. S.; Keglevich, G. *Heteroat. Chem.* **2007**, *18*, 759−766. (q) Yamabe, S.; Yamazaki, S. *J. Org. Chem.* **2007**, *72*, 3031−3041. (r) Alvarez-Idaboy, J. R.; Reyes, L. *J. Org. Chem.* **2007**, *72*, 6580−6583. (s) Alvarez-Idaboy, J. R.; Reyes, L.; Mora−Diez, N. *Org. Biomol. Chem.* **2007**, *5*, 3682−3689. (t) Reyes, L.; Alvarez-Idaboy, J. R.; Mora-Diez, N. *J. Phys. Org. Chem.* **2009**, *22*, 643−649. (u) Mora-Diez, N.; Keller, S.; Alvarez-Idaboy, J. R. *Org. Biomol. Chem.* **2009**, *7*, 3682−3690. (v) Xu, S.; Wang, Z.; Li, Y.; Zhang, X.; Wang, H.; Ding, K. *Chem.—Eur. J.* **2010**, *16*, 3021−3035. (w) Liu, B.; Meng, X.-G.; Li, W.-Y.; Zhou, L.-C.; Hu, C.-W. *J. Phys. Chem. A* **2012**, *116*, 2920−2926. (x) Reyes, L.; Díaz-Sánchez, C.; Iuga, C. *J. Phys Chem. A* **2012**, *116*, 7712−7717.

(12) Frisch, M. J.; Trucks, G. W.; Schlegel, H. B.; Scuseria, G. E.; Robb, M. A.; Cheeseman, J. R.; Scalmani, G.; Barone, V.; Mennucci, B.; Petersson, G. A.; Nakatsuji, H.; Caricato, M.; Li, X.; Hratchian, H. P.; Izmaylov, A. F.; Bloino, J.; Zheng, G.; Sonnenberg, J. L.; Hada, M.; Ehara, M.; Toyota, K.; Fukuda, R.; Hasegawa, J.; Ishida, M.; Nakajima, T.; Honda, Y.; Kitao, O.; Nakai, H.; Vreven, T.; Montgomery, J. A., Jr.; Peralta, J. E.; Ogliaro, F.; Bearpark, M.; Heyd, J. J.; Brothers, E.; Kudin, K. N.; Staroverov, V. N.; Kobayashi, R.; Normand, J.; Raghavachari, K.; Rendell, A.; Burant, J. C.; Iyengar, S. S.; Tomasi, J.; Cossi, M.; Rega,

N.; Millam, J. M.; Klene, M.; Knox, J. E.; Cross, J. B.; Bakken, V.; Adamo, C.; Jaramillo, J.; Gomperts, R.; Stratmann, R. E.; Yazyev, O.; Austin, A. J.; Cammi, R.; Pomelli, C.; Ochterski, J. W.; Martin, R. L.; Morokuma, K.; Zakrzewski, V. G.; Voth, G. A.; Salvador, P.; Dannenberg, J. J.; Dapprich, S.; Daniels, A. D.; Farkas, Ö.; Foresman, J. B.; Ortiz, J. V.; Cioslowski, J.; Fox, D. J. *Gaussian 09*, revision C.01; Gaussian, Inc.: Wallingford, CT, 2009.

(13) Hehre, W. J.; Radom, L.; von Ragué Schleyer, P.; Pople, J. A. *Ab Initio Molecular Orbital Theory*; Wiley: New York, 1986, and references cited therein.

(14) (a) Becke, A. D. *Phys. Rev.* **1988**, *A38*, 3098−3100. (b) Becke, A. D. *J. Chem. Phys.* **1993**, *98*, 1372−1377. (c) Becke, A. D. *J. Chem. Phys.* **1993**, *98*, 5648−5652. (d) Lee, C.; Yang, W.; Parr, R. G. *Phys. Rev.* **1988**, *B37*, 785−788.

(15) Zhao, Y.; Truhlar, D. G. *J. Phys. Chem. A* **2004**, *108*, 6908−6918.

(16) (a) Onsager, L. *J. Am. Chem. Soc.* **1936**, *58*, 1486−1493. (b) Tomasi, J.; Mennucci, B.; Cammi, R. *Chem. Rev.* **2005**, *105*, 2999−3093.

(17) (a) Miertus, S.; Scrocco, E.; Tomasi, J. *Chem. Phys.* **1981**, *55*, 117−129. (b) Miertus, S.; Tomasi, J. *Chem. Phys.* **1982**, *65*, 239−245.

(18) Reed, A. E.; Weinstock, R. B.; Weinhold, F. *J. Chem. Phys.* **1985**, *83*, 735−746.

(19) Jensen, F. R.; Bushweller, C. H. *Adv. Alicyclic Chem.* **1971**, *3*, 139−195.